ASM Sc. J., 18, 2023

https://doi.org/10.32802/asmscj.2023.1353

# Modelling Backscattered Light in Fibre Optic Based on Light Propagation

M.H. Jamaludin[1,2], W.Z. Wan Ismail[1*], F.S.N. Mohd Romzi[1], K.N. Zainul Ariffin[1] and S. Suhaimi[3]

[1]*Advanced Devices and System (ADS), Faculty of Engineering and Build Environment, Universiti Sains Islam Malaysia, 71800 Nilai, Negeri Sembilan, Malaysia*

[2]*Centre of Excellence for Engineering and Technology JKR (CREaTE), Jabatan Kerja Raya Malaysia, 78000, Alor Gajah, Melaka, Malaysia*

[3]*Faculty of Science and Technology, Universiti Sains Islam Malaysia, 71800 Nilai, Negeri Sembilan, Malaysia*

Nowadays, fibre optic sensors have been widely used to detect temperature, pressure, vibration and other physical properties. To design high performance fibre optics sensors, sensing elements such as light propagation need to be investigated for parameters such as absorbance, transmittance and scattering. In this study, the backscattered light is studied and modelled using MATLAB based on Brillouin and Rayleigh scattering. The scattering effects on the output power and Stokes power are clearly seen where both powers reduce with the increase of fibre length. The Rayleigh power in terms of Coherent Rayleigh Noise is studied where broader source linewidth, higher spatial resolution and lower group velocity produce less noise. The less fluctuation due to noise can be attributed to the less temporal and spatial fluctuations of the optical pump power or pump current. The output from this research can benefit experimental studies to design fibre optic sensors in future.

**Keywords:** Brillouin scattering; Rayleigh scattering; Coherent Rayleigh Noise; Light propagation

## I. INTRODUCTION

Nowadays, sensors are significant in our daily life. Fibre optic sensors have gained tremendous growth in commercial sector due to its excellent features such as high sensitivity, mobility and robustness (Masoudi & Newson, 2016, 2017). Basically, fibre optic sensor comprises of optical source, optical fibre, transducer, optical detector and end-processing devices. This sensor uses fibre optic as a sensing element and it is used to measure various parameters (physical, chemical or biological) that changes some optical property of the system (Shizhuo Yin & Paul B. Ruffin, 2019). In general, sensing in fibre optic is based on the changes in one or more light wave properties such as intensity, phase, frequency, and polarization (Sabri *et al.*, 2013).

When high-power incident light shines the optical fibre, the light will propagate and scatter along the fibre, producing Brillouin, Rayleigh and Raman scattering effects. Any changes in physical parameters such as strain and temperature will modulate the signal propagating through the fibre. Thus, sensing along fibre can be performed by measuring the variation resulted by such modulation.

Light propagation in a fibre depends on properties of incident light and optical properties of medium (Bao & Chen, 2012). Light propagation consists of absorption, scattering, and transmission (Meretska *et. al.*, 2017; Kamil *et. al.*, 2021a). When the light is interacted with any medium, the light is either absorbed or remains unabsorbed within the medium. The unabsorbed light will be transmitted in two ways, either reemitted or emerged from other side. The light also may change its direction or stay to travel in its current path. The absorption of light is defined as the disappearance of photon after it hits particle or molecule whereas light scattering refers to a change of light direction from a straight trajectory when it is passing a non-uniform material (Øgendal, 2016). Studies on light propagation can consist of

*Corresponding author's e-mail: drwanzakiah@usim.edu.my

free space optics, lasers and analysis of milk (Zainurin *et. al.*, 2020; Wan Ismail *et. al.*, 2020; Kamil *et al.*, 2021b).

If the wavelength of the light is distant from a medium resonance, a time-dependent polarization dipole will be generated by the electric field (Bao & Chen, 2012). If the medium is completely homogeneous, the phase relationship of the transmitted waves only produces a forward scattered beam. Medium with impurities, causes backscattering which changes the direction of transmitted light. If any strain or temperature changes in the fibre, density fluctuation occurs, affecting the characteristics of the backscattered light (Soga & Luo, 2018).

The backscattering effect was initially studied by (Kapron *et. al.,* 1972; Smith, 1972; Lines, 1984). Backscattering effects were used to characterise loss and defective properties in fibre, which resulting in the development of Optical Time Domain Reflectometry, OTDR (Barnoski & Jensen, 1976).

The backscattered light which propagates along a fibre consists of Rayleigh, Raman and Brillouin scattering. The light travels back to the initial position, detected by the receiver. The elastically scattered light is captured within the numerical aperture of the fibre in a backward direction as the pulse travels and subsequently is transmitted back to the coupler. Backscattered lights are produced at each point of the fibre whenever a light pulse is launched. If the backscattered light is nearer to the initial point, it will come back faster and quicker (Mukhzeer Mohamad Shahimin, 2013).

Basically, distributed sensing uses Brillouin scattering, as it is capable to continuously extract data such as pressure, strain and temperature along the fibre. Besides the Stimulated Brillouin Scattering (SBS), there is a linear scattering, known as Rayleigh scattering. The nonlinear Brillouin scattering has a power threshold above the linear Rayleigh scattering. Thus, the coherent fluctuating backscattered signal will corrupt the Brillouin signal (Mukhzeer Mohamad Shahimin, 2013).

In addition, the fibre optic sensor is not only limited by receiver noise. The Rayleigh backscattered radiation, instead, inherits a noise feature that is caused by the interference among a large number of light waves backscattered at different positions in the fibre, which is called fading noise or Coherent Rayleigh Noise (CRN). This noise affects the pure output power as it is able to degrade the overall signal-to-noise ratio and therefore causes a serious limitation to achieve resolution (De Souza, 2006). CRN is inherent to Rayleigh backscattered radiation. Therefore, the effects of the Rayleigh noise must be taken into consideration to obtain an accurate response of the sensor.

Recent studies of backscattered light in fibre optic involve Rayleigh scattering for static and dynamic strain measurement (Coscetta, 2021a), backscattering with engineered nanoparticle (Fuertes, 2021; Lu, 2022), integrated system with Brillouin/Rayleigh system for measuring multi-parameter in fibre optics (Coscetta, 2021b) and effect of double Rayleigh backscattering on fibre-optic radio frequency transfer (Li Q, 2021). Previous studies did not study Brillouin and Rayleigh scattering with CRN in details. Here, we model backscattered light based on light propagation involving Brillouin and Rayleigh scattering effects. Both scattering phenomena affect the output and Stokes power. The effects of Coherent Rayleigh Noise in terms of source linewidth, spatial resolution and group velocity have also been investigated.

## II. METHODOLOGY

Figure 1 shows a flow chart of the modelling used in this study.

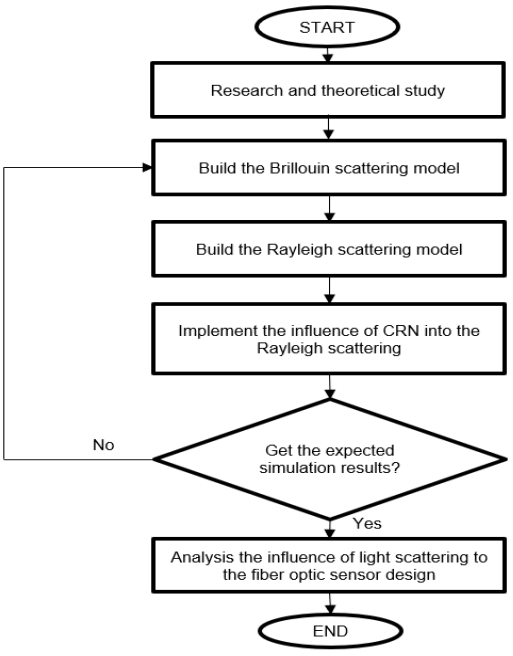


Figure 1. Flow chart of the project

### *A. Stimulated Brillouin Scattering (SBS)*

Principally, there are two methods to simulate Stimulated Brillouin scattering in optical fibre; (1) Initial Value Problems (IVP), and (2) Boundary Value Problems.

The characteristics of SBS in fibre optic sensor can be studied using the rate equations, as shown in Equation (1):

$$\frac{dI_p}{dz} = -g_B I_P I_S - \alpha I_P$$

$$\frac{dI_S}{dz} = -g_B I_P I_S + \alpha I_S \quad (1)$$

where $I_P$, $I_S$, $g_B$, and α are the Stokes intensity, the pump intensity, the Brillouin gain coefficient and the losses at pump/Stokes frequencies, respectively.

The modelling of Brillouin scattering effect is done using Equation (1), that relates the forward signal with the backscattered signal. MATLAB is used as a platform to model the Brillouin scattering.

In the modelling, we assume the length of the medium is *L* (*z=0* to *L*) and pump laser, $I_P$ goes into *z=0* and the Stokes seed laser, $I_S$ goes into *z=L*. Thus, the initial conditions for $I_P$ is $I_P(0)$ and $I_S$ is $I_S(L)$. $I_P$ should be calculated from *z=0* to *z=L* and $I_S$ should be calculated from z=L to z=0. The parameter values used in the modelling are given in Table 1 (Dossou, 2008).

Table 1. Parameter values for SBS simulation

| Parameters | Values | Unit |
|---|---|---|
| Initial pump power | 4.2 | Mw |
| Initial Stokes power | 1.726 | Mw |
| Brillouin gain | $1.2\text{x}10^{-11}$ | m/W |
| Effective area core | 86 | $\mu m^2$ |
| Laser wavelength | 1550 | Nm |
| Attenuation coefficient | 0.217 | dB/km |

Since the rate equations of the SBS are the Ordinary Differential Equations (ODEs), the ode45 is used to solve the equation. It performs a direct numerical integration of a set of differential equations.

### *B. Rayleigh Scattering and Coherent Rayleigh Noise (CRN)*

The modelling of Rayleigh scattering in optical fibres is divided into two parts; (1) backscattered Rayleigh power without CRN, and (2) backscattered Rayleigh power with CRN. In the modelling, the Rayleigh equation is firstly represented as a function. The backscatter power of Rayleigh scattering can be presented by Equation (2):

$$P_R(t) = \frac{1}{2} P_i S \gamma_R w_0 v_g \exp(-\gamma_R v_g t) = P_R(0) \exp(-\gamma_R v_g t) \quad (2)$$

Here, we assume silica fibre at λ=1.55 μm, numerical aperture (NA)=0.12, n=1.46, and $\gamma_R=4.6\text{x}10^{-5}$ $m^{-1}$. By substituting these values, the backscattered power formula can be simplified as in Equation (3):

$$P_R(t) = 7.8E_P \exp(-\gamma_R v_g t) = 7.8E_P \exp(-2\gamma_R x) \quad (3)$$

where $E_p$ is the pulse in unit Joule (J).

In the simulation, the parameter values are set based on Table 2 (Shahimin, 2013).

Table 2. Parameter values for Rayleigh scattering simulation

| Parameters | Values | Unit |
|---|---|---|
| Rayleigh scattering coefficient, $\gamma_R$ | $4.6\text{x}10^{-5}$ | $m^{-1}$ |
| Initial backscattered Rayleigh power, Pro | $1\text{x}10^{-3}$ | Watts |

Then, the influence of CRN are considered in the modelling. A fraction of the Rayleigh signal, fCRN can be shown in Equation (4):

$$f_{CRN} = \sqrt{\frac{v_g}{4\Delta z \Delta v}} \quad (4)$$

where $v_g$, Δz and Δv are the group velocities of light in fibre, the spatial resolution and the frequency-shifted bandwidth of a source, respectively. Parameters used in the modelling are set based on Table 3 (Shahimin, 2013).

Table 3. Parameter values for CRN simulation

| Parameters | Values | Unit |
|---|---|---|
| Group velocity, *vg* | $2\text{x}10^8$ | m/s |
| Signal linewidth, *dv* | $0.3\text{x}10^9$ | Hz |
| Spatial resolution, *dz* | 40 | M |

The root-mean-square (rms) value of the percentage CRN is firstly calculated using equation of fCRN and is then multiplied with the MATLAB code “randn”. This “randn” function generates arrays of random numbers whose elements are normally distributed with mean 0 and variance 1, and the “randn('state',0)” resets the generator to its initial state. Thus, in this case, the “randn” randomly generates numbers with mean zero, variance one and standard deviation one to imitate CRN.

As the CRN depends on the parameters in Equation (4), the modelling is performed to determine the variation of CRN with source linewidth, spatial resolution and group velocity parameters. These parameters are investigated to observe their effects on the CRN.

## III. RESULTS AND DISCUSSION

The modelling and data analysis are given in terms of power and scattered signal.

### *A. Stimulated Brillouin Scattering*

The output power in terms of fibre length is shown in Figure 2. It is clearly shown that the output power gradually decreases as the fibre length increases. Thus, the higher of the signal power, the optimum the fibre length is shorter. We attribute that to the less attenuation in the shorter fibre.

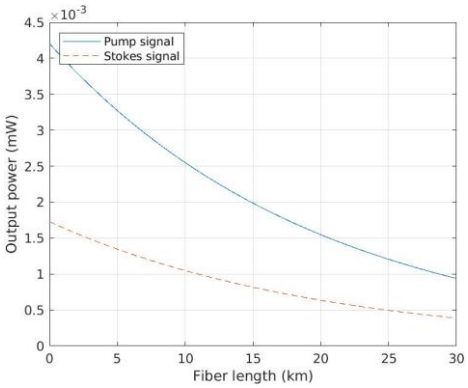


Figure 2. Simulation of pump and Stokes signal over 30km-long optical fibre using MATLAB

The attenuation of light in a fibre depends on initial power stokes where the attenuation will decrease as the initial power increases. (Bouyahi *et al.*, 2016). The initial Stokes intensity are varied as 74.7 mW, 48.6 mW and 9.12 mW. Figure 3 shows that the Stokes signal depends on initial intensity. The curves gradually reach zero as the fibre length increases.

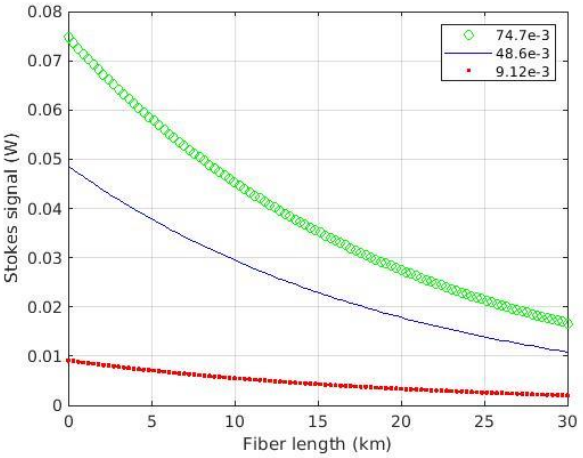


Figure 3. Stokes signal as a function of fibre length

In addition, the transmitted power and Stokes power can also be plotted as a function of the launched pump intensity, as shown in Figure 4 and Figure 5, respectively. The launched power is set up to 10 mW.

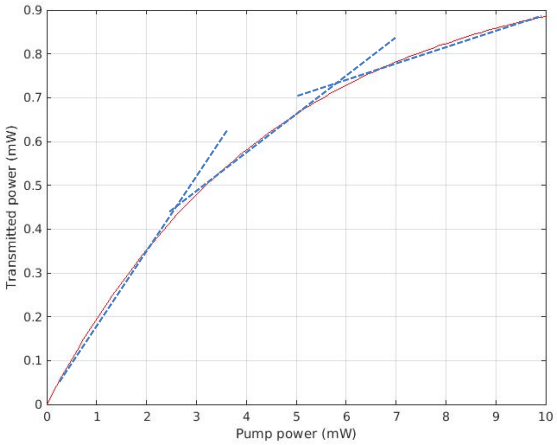


Figure 4. Transmitted power as a function of the launched pump intensity. The dashed blue line shows the slope of the graph.

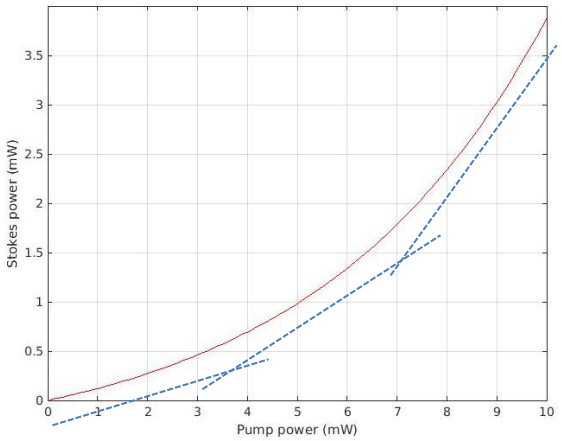


Figure 5. Stokes power as a function of the launched pump intensity. The dashed blue line shows the slope of the graph.

Figure 4 clearly shows that the slope of the transmitted power reduces as the launched power increases. It also depicts that the optical power will reach saturation by increasing the launched power. Thus, the input power limit should be limited (Mukhzeer Mohamad Shahimin, 2013).

Meanwhile, Figure 5 shows that the Stokes power is increasing with the launched power. In addition, the graph also shows that the slope increases with the increase of the launched power. We attribute that to the decrease of gain with a larger input power.

### *B. Rayleigh Scattering and Coherent Rayleigh Noise (CRN)*

The simulation result of Rayleigh power without CRN is shown in Figure 6(a), whereas the simulation result of Rayleigh power with the influence of CRN is shown in Figure 6(b). Figure 6 shows that the CRN affects the Rayleigh power where the signal attenuates and degrades the signal-to-noise ratio.

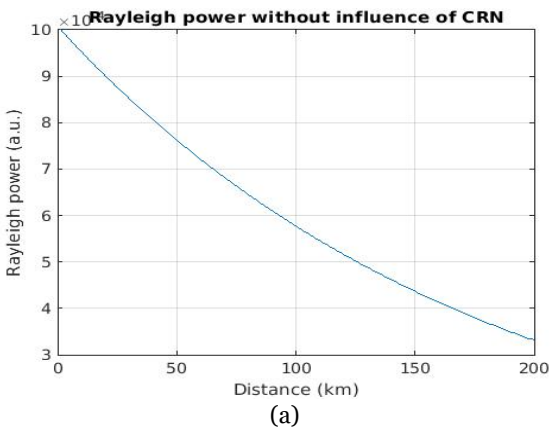


(a)

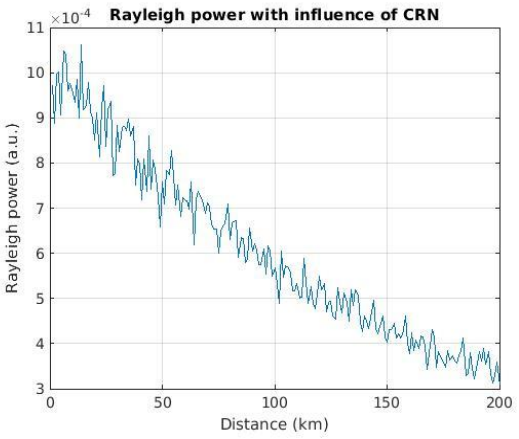


(b)

Figure 6. The Rayleigh power (a) without CRN, and (b) with CRN

Then, the CRN is investigated based on source linewidth, spatial resolution and group velocity. Based on Equation (4), the values of fCRN are calculated theoretically. In the simulation, the values of source linewidth, spatial resolution and group velocity are varied. Theoretical percentages of CRN for three different source linewidths are shown in Table 4.

Table 4. Theoretical CRN based on various parameters

| **Parameters** | **Theoretical % CRN** |
|---|---|
| $\Delta v$ = 1.3 GHz, $\Delta z$ = 40 m, $v_g$ = 2x10$^8$ m/s | 3.1 |
| $\Delta v$ = 30 GHz, $\Delta z$ = 40 m, $v_g$ = 2x10$^8$ m/s | 0.64 |
| $\Delta v$ = 320 GHz, $\Delta z$ = 40 m, $v_g$ = 2x10$^8$ m/s | 0.19 |
| $\Delta v$ = 30 GHz, $\Delta z$ = 10 m, $v_g$ = 2x10$^8$ m/s | 1.3 |
| $\Delta v$ = 30 GHz, $\Delta z$ = 40 m, $v_g$ = 2x10$^8$ m/s | 0.65 |
| $\Delta v$ = 30 GHz, $\Delta z$ = 140 m, $v_g$ = 2x10$^8$ m/s | 0.34 |
| $\Delta v$ = 30 MHz, $\Delta z$ = 40 m, $v_g$ = 0.2x10$^8$ m/s | 6.45 |
| $\Delta v$ = 30 MHz, $\Delta z$ = 40 m, $v_g$ = 2x10$^8$ m/s | 20.4 |
| $\Delta v$ = 30 MHz, $\Delta z$ = 40 m, $v_g$ = 20x10$^8$ m/s | 64.5 |

The simulation results of the normalised Rayleigh scattering effect with varied source linewidth are presented in Figure 7.

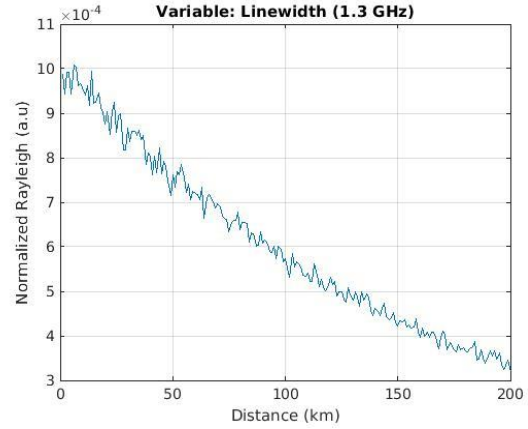


(a)

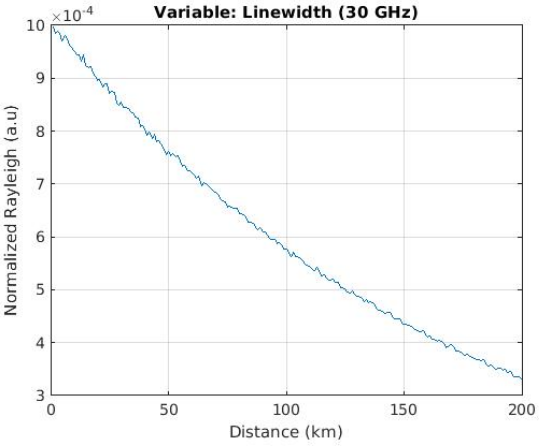


(b)

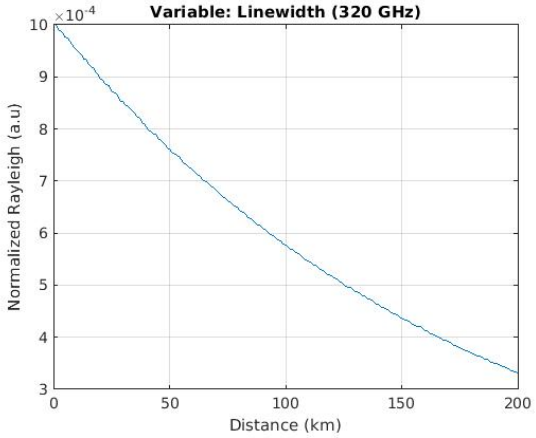


(c)

Figure 7. The normalised backscattered Rayleigh signal with (a) – (c) linewidths of 1.3 GHz, 30 GHz, 320 GHz

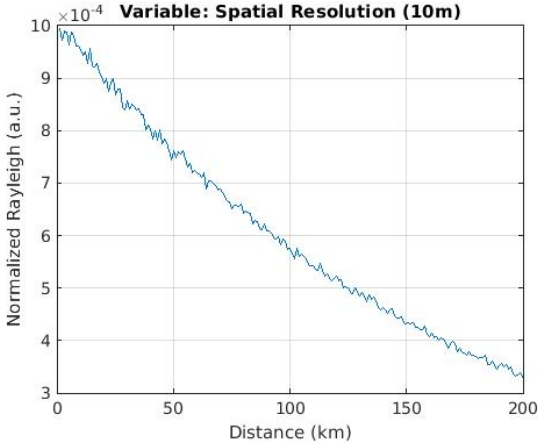


(a)

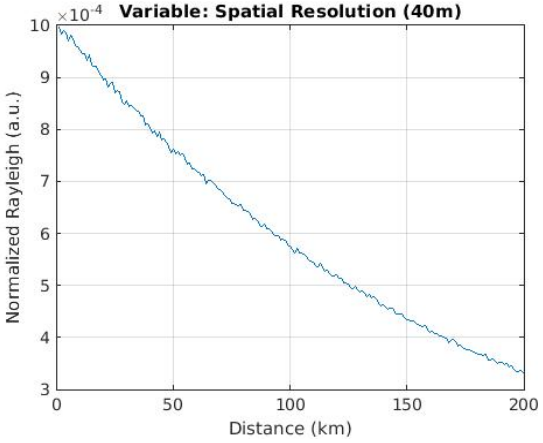


(b)

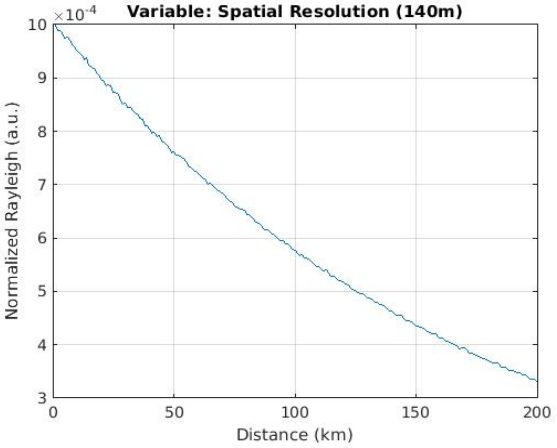


(c)

Figure 8. The normalised backscattered Rayleigh signal with (a) – (c) spatial resolution of 10m, 40m, 140m

Figure 8 shows the simulation results of the normalised Rayleigh scattering effect with varied spatial resolution.

Figure 9 shows the simulation results of the normalised Rayleigh scattering effect with varied group velocity.

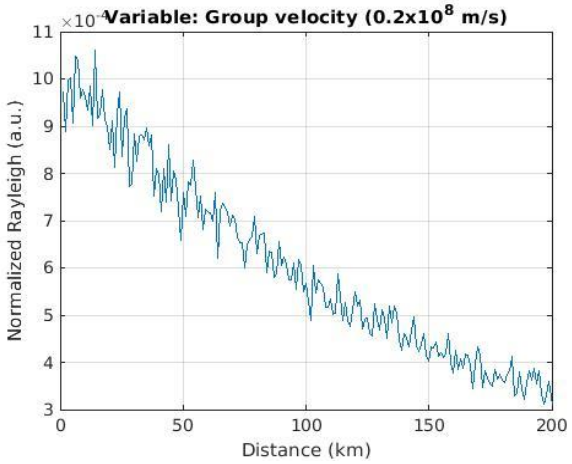


(a)

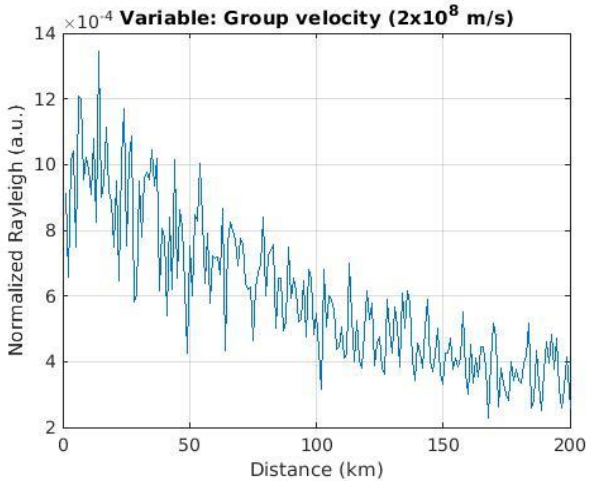


(b)

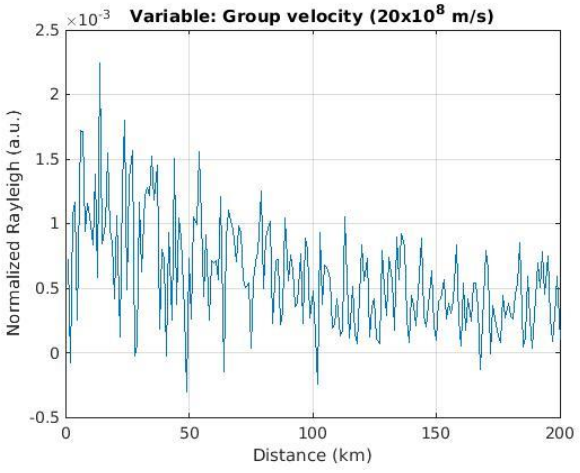


(c)

Figure 9. The normalised backscattered Rayleigh signal with *(a) – (c)* group velocity of $0.2x10^8 ms^{-1}$, $2x10^8 ms^{-1}$, $20x10^8 ms^{-1}$

The simulation results corresponds to the theoretical results presented in Table 4, which are calculated using Equation (4). Figures 7, 8 and 9 show the backscattered Rayleigh signals obtained based on parameters in Table 4.

Figure 7(a)-(c) shows the influence of source linewidths to the amplitude of CRN. In the simulation, the values of source linewidth are varied from 1.3GHz to 320GHz, while the value of other parameters are set as constant. It is clearly shown that the amplitude of CRN decreases with the increasing source linewidth. Meanwhile, spatial resolution gives slight changes on the amplitude of CRN (Figure 8(a)-(c)). In the simulation, the values of spatial resolution are varied as 10m, 40m and 140m. The results show that the amplitude of CRN decreases with increasing spatial resolution. The influence of group velocity on the amplitude of CRN is also investigated (Figure 9(a)-(c)). The values of group velocity are varied as $0.2x10^8$ $ms^{-1}$, $2x10^8$ $ms^{-1}$ and $20x10^8$ $ms^{-1}$, while the other parameters are fixed as constant. The graphs show that less group velocity can reduce the amplitude of CRN. Thus, the effects of CRN on the backscattered Rayleigh signal is clearly shown, where the fluctuation in the backscatter trace becomes less significant for broader source linewidth, higher spatial resolution and lower group velocity. We attribute that to the less temporal and spatial fluctuations of the optical pump power or pump current.

## IV. CONCLUSION

In conclusion, this research studies the characteristics of the backscattered signal in fibre optic sensor. The characteristics of Brillouin scattering and Rayleigh scattering in optical fibres are studied through simulation using MATLAB. The influence of Coherent Rayleigh Noise (CRN), a dominant noise source is also considered in the simulation where lower group velocity, broader source linewidth and higher spatial resolution can produce less noise. Mathematical models and equations are presented and the analysis of the simulations is clearly presented. We found that output power and Stokes power reduce with the increase of fibre length. Thus, the findings from this study are useful to be applied in designing fibre optic sensors.

## V. ACKNOWLEDGEMENT

We acknowledge the Ministry of Higher Education Malaysia under FRGS grant (FRGS/1/2021/WAB02/USIM/02/1) and the Faculty of Engineering and Built Environment, Universiti Sains Islam Malaysia (USIM) for the funding and support.

## VI. REFERENCES


Bao, X & Chen, L 2012, 'Recent Progress in Distributed Fiber Optic Sensors', Sensors (Switzerland), vol. 12, no. 7, pp. 8601–8639. doi: 10.3390/s120708601.

Barnoski, MK & Jensen, SM 1976, 'Fiber waveguides: a novel technique for investigating attenuation characteristics', Applied Optics, vol. 15, no. 9, pp. 2112. doi: 10.1364/ao.15.002112.

Bouyahi, M *et al.* 2016, 'Modeling the brillouin spectrum by measurement of the distributed strain and temperature', Optical and Quantum Electronics, Springer US, vol. 48, no. 2. doi: 10.1007/s11082-016-0395-3.

Coscetta, A, Catalano, E, Cerri E, Oliveira, R, Bilro, L, Zeni, L, Cennamo, N & Minardo, A 2021a, 'Distributed Static and Dynamic Strain Measurements in Polymer Optical Fibers by Rayleigh Scattering', Sensors, vol. 21, pp. 5049.

Coscetta, A, Catalano, E, Cerri E, Cennamo, N, Zeni, L & Minardo, A 2021b, 'Hybrid Brillouin/Rayleigh sensor for multiparameter measurements in optical fibers', Optics Express, vol. 29, no. 15, pp. 24025.

Dossou, AGM & Szriftgiser, P 2008, 'Theoretical study of Stimulated Brillouin Scattering (SBS) in polymer optical fibres,' in Proceedings Symposium IEEE/LEOS, 2008.

Fuertes, V, Grégoire, N, Labranche, P, Gagnon, S, Wang, R, Ledemi, Y, LaRochelle, S & Messaddeq Y 2021, 'Engineering nanoparticle features to tune Rayleigh scattering in nanoparticles-doped optical fibers', Scientific Reports, vol. 11, pp. 9116.

Kamil, NAIM, Noraini ZS, Wan Ismail, WZ, Ismail I, Jamaludin J, Balakrishnan SR 2021a, 'Investigating the Quality of Milk using Spectrometry Technique and Scattering Theory', Engineering, Technology & Applied Science Research, vol. 11, no. 3, pp. 71111.

Kamil, NAIM, Wan Ismail, WZ, Ismail, I, Jamaludin, J, Hanasil, NS & Raja Ibrahim, RK 2021b, 'Analysis of Milk from Different Sources Based on Light Propagation and Random Laser Properties', Photonics, vol. 8, no. 11, pp. 486.

Kapron, FP, Maurer, RD & Teter, MP 1972, 'Theory of Backscattering Effects in Waveguides', Applied Optics, vol. 11, no. 6, pp. 1352. doi: 10.1364/ao.11.001352.

Lines, ME 1984, 'Scattering losses in optic fiber materials. I. A new parametrization', Journal of Applied Physics, vol. 55, no. 11, pp. 4052–4057. doi: 10.1063/1.332994.

Li, Q, Hu, L, Chen, J & Wu, G 2021, 'Studying the Double Rayleigh Backscattering Noise Effect on Fiber-Optic Radio Frequency Transfer', IEEE Photonics Journal, vol. 13, no. 2, pp. 7100210.

Lu, Z, Robine, T, Molardi, C, Pigeonneau, F, Tosi, D & Wilfried Blanc 2022, 'Toward Engineered Nanoparticle-Doped Optical Fibers for Sensor Applications', Frontiers in Sensor Applications, vol. 2, p. 805351.

Masoudi, A & Newson, TP 2016, 'Contributed Review: Distributed optical fibre dynamic strain sensing', Review of Scientific Instruments, vol. 87, no. 1. doi: 10.1063/1.4939482.

Masoudi, A & Newson, TP 2017, 'Analysis of distributed optical fibre acoustic sensors through numerical modelling', Optics Express, vol. 25, no. 25, pp. 32021. doi: 10.1364/oe.25.032021.

Meretska, ML *et al.* 2017, 'Analytical modeling of light transport in scattering materials with strong absorption', Optics Express, vol. 25, no. 20, pp. A906. doi: 10.1364/oe.25.00a906.

Mukhzeer Mohamad Shahimin, SA 2013, Modeling of Fiber Optic Sensor Based on Backscattered Signal Using MATLAB, Edited by Penerbit Universiti Malaysia Perlis, Perpustakaan Negara Malaysia.

Øgendal, L 2016, 'Light Scattering a brief introduction', University of Copenhagen, (February), pp. 3–4.

Sabri, N *et al.* 2013, 'Toward optical sensors: Review and applications', Journal of Physics: Conference Series, vol. 423, no. 1. doi: 10.1088/1742-6596/423/1/012064.

Shizhuo Yin, Paul B Ruffin, FTSY 2019, Fiber Optic Sensors, 2nd edn, CRC Press.

Smith, RG 1972, 'Optical Power Handling Capacity of Low Loss Optical Fibers as Determined by Stimulated Raman and Brillouin Scattering', Applied Optics, vol. 11, no. 11, pp. 2489. doi: 10.1364/ao.11.002489.

Soga, K & Luo, L 2018, 'Distributed fiber optics sensors for civil engineering infrastructure sensing', Journal of Structural Integrity and Maintenance, Taylor & Francis, vol. 3, no. 1, pp. 1–21. doi: 10.1080/24705314.2018.1426138.

De Souza, K 2006, 'Significance of coherent Rayleigh noise in fibre-optic distributed temperature sensing based on spontaneous Brillouin scattering', Measurement Science and Technology, vol. 17, no. 5, pp. 1065–1069. doi: 10.1088/0957-0233/17/5/S21.

Wan Ismail, WZ, Hurot, C & Dawes, J 2020, 'Properties of Random Lasers in a hollow core photonic crystal fiber',

Laser Physics, vol. 30, no. 3, pp. 035002.

Zainurin, SN, Ismail, I, Saulaiman, US, Wan Ismail, WZ, Mustafa, FH, Sahrim, M, Jamaluddin, J & Balakrishnan, SR 2020, 'A study on Malaysia atmospheric effect on radio over free space optic through radio frequency signal and light propagation in fiber for future communication development', AIP Conference Proceedings, vol. 2203, no. 1 pp. 020018.